Inorganic Chemistry

Communication

pubs.acs.org/IC

Mononuclear Ruthenium–Water Oxidation Catalysts: Discerning between Electronic and Hydrogen-Bonding Effects

Somnath Maji,[†] Isidoro López,[†] Fernando Bozoglian,[†] J. Benet-Buchholz,[†] and Antoni Llobet*[,†,‡]

[†]Institute of Chemical Research of Catalonia, Avinguda Països Catalans 16, 43007 Tarragona, Spain

[‡]Departament de Química, Universitat Autònoma de Barcelona, Cerdanyola del Vallès, 08193 Barcelona, Spain

Supporting Information

ABSTRACT: New mononuculear complexes of the general formula $[Ru(trpy)(n,n'\text{-}F_2\text{-}bpy)X]^{m+}$ [$n = n' = 5$, X = Cl ($\mathbf{3}^+$) and H_2O ($\mathbf{5}^{2+}$); $n = n' = 6$, X = Cl ($\mathbf{4}^+$) and H_2O ($\mathbf{6}^{2+}$); trpy is 2,2′:6′:2″-terpyridine] have been prepared and thoroughly characterized. The 5,5′- and 6,6′-F_2-bpy ligands allow one to exert a remote electronic perturbation to the ruthenium metal center, which affects the combination of species involved in the catalytic cycle. Additionally, 6,6′-F_2-bpy also allows through-space interaction with the Ru–O moiety of the complex via hydrogen interaction, which also affects the stability of the different species involved in the catalytic cycle. The combination of both effects has a strong impact on the kinetics of the catalytic process, as observed through manometric monitoring.

Since the discovery by Zong and Thummel[1] that mononuclear ruthenium complexes were also active as water oxidation catalysts, there has been a large development in the field based on these types of complexes. In 2008, Meyer et al.[2] offered a mechanistic description of how the water oxidation occurred at a molecular level, where the O–O bond formation is proposed to occur based on the water nucleophilic attack pathway. This description has now been adopted to many mononuclear ruthenium complexes but also to those of iridium and other first-row transition metals, where water oxidation catalysis is claimed to proceed in a molecular manner.[3] Later on, Berlinguette and co-workers studied the strong influence that electronic perturbation of the metal center exerted through remote positions of the ligands over the whole water oxidation catalysis process.[4] Recent reports by Yagi and Fujita have shown how the presence of a nitrogen lone pair can influence the reactivity in isomeric 2-(2-pyridyl)-1,8-naphthyridine complexes.[5] In order to evaluate the electronic and hydrogen-bonding effects individually, we have designed complexes containing ligands that allow through-space interaction with the active $RuOH_2$ entourage in mononuclear complexes, in combination with others that only exert remote electronic perturbation.

In the present paper, we report a new family of complexes of the general formula $[Ru(trpy)(n,n'\text{-}F_2\text{-}bpy)X]^{m+}$ [$n = n' = 5$, X = Cl ($\mathbf{3}^+$) and H_2O ($\mathbf{5}^{2+}$); $n = n' = 6$, X = Cl ($\mathbf{4}^+$) and H_2O ($\mathbf{6}^{2+}$)] that allow us to discern and quantify the electronic and hydrogen-bonding effects. Additionally, we report their activity as water oxidation catalysts and compare them with the reference complex $[Ru(tpry)(bpy)OH_2]^{2+}$ ($\mathbf{2}^{2+}$).[6]

The synthetic strategy followed for the synthesis of complexes **3**–**6** uses $[RuCl_3(tpry)]$ (**1**) as the starting material and is similar to the one used for the preparation of $\mathbf{2}^{2+}$. Synthetic details, together with a complete structural and spectroscopic characterization, are presented as Supporting Information (SI). An ORTEP plot of the X-ray structure of $\mathbf{6}^{2+}$ is given in Figure 1, whereas that of $\mathbf{5}^{2+}$ is presented as SI. In

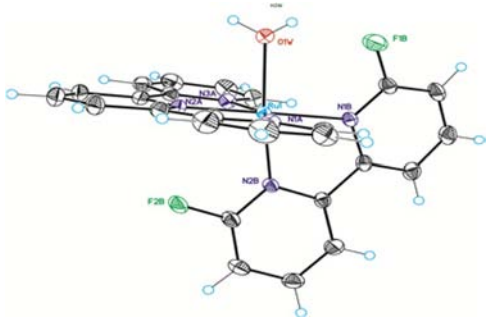

Figure 1. ORTEP plot (50% probability) of the crystal structure of complex $\mathbf{6}^{2+}$. Color code: Ru, cyan; N, navy blue; F, green; O, red; H, blue empty circles. Interesting metric parameters: d(H2W–F1B) = 2.32 Å; d(F1B–O1W) = 2.63 Å; ∠(O1W–H2W–F1B) = 100.7°; the dihedral angle between the pyridyl moieties of 6,6′-F_2-bpy is 11.6°.

both cases, the Ru center presents an octahedrally distorted geometry around the metal center, and the bond distances and angles are unremarkable except for the hydrogen-interaction of the F atom with the aqua group in $\mathbf{6}^{2+}$. This interaction is also responsible for rotation of one of the pyridyl groups of bpy, generating a dihedral angle of 11.6°, needed to be able to accommodate the F atom of the bpy ligand so close to the aqua group. In turn, this close and rigid interaction will ensure that all of the potential species that can be generated along the catalytic cycle will have an interaction with this group. The redox properties of complexes $\mathbf{5}^{2+}$ and $\mathbf{6}^{2+}$ were investigated with cyclic voltammetry and differential pulse voltammetry experiments in water at different pH values and are reported in Table 1, Figure 2, and the SI. The presence of the F substituent at the bpy ligand has a dramatic influence on the electronic structure of the metal center in the sense that for these

Received: December 25, 2012
Published: March 21, 2013

   dx.doi.org/10.1021/ic3028176 | *Inorg. Chem.* 2013, 52, 3591–3593

Table 1. Thermodynamic and Catalytic Data for 5^{2+} and 6^{2+} and for Related Ruthenium–Water Complexes Described in the Literature at pH = 7.0

		$E_{1/2}$ (V) vs SSCE								
entry	complex[a]	IV/III	III/II	IV/II	V/IV	$\Delta E_{1/2}$[b]	$pK_{a,II}$[c]	$pK_{a,III}$[c]	$TOF_i \times 10^3$[d]	ref
1	$[Ru(trpy)(bpy)(H_2O)]^{2+}$	0.59	0.48	0.54	1.62	110	9.8	1.7	15.1 (18.3)	Tw[e]
2	$[Ru(trpy)(6,6'\text{-}F_2\text{-}bpy)(H_2O)]^{2+}$			0.56[f]	1.69		10.4		1.7 (7.8)	Tw
3	$[Ru(trpy)(5,5'\text{-}F_2\text{-}bpy)(H_2O)]^{2+}$			0.54[f]	1.68		9.0		4.3 (13.0)	Tw
5	$[Ru(CNC)(bpy)(H_2O)]^{2+}$	0.50	0.45	0.48		50	10.9	2.3		7
6	$[Ru(trpy)(bpm)(H_2O)]^{2+}$			0.62[f]			9.7			2
7	$[Ru(damp)(bpy)(H_2O)]^{2+}$	0.44	0.30	0.37		140	11.5			8

[a]Ligand abbreviations: CNC is 2,6-bis(butylimidazol-2-ylidene)pyridine; bpm is 2,2′- bipyrimidine; damp is 2,6-bis[(dimethylamino)methyl]-pyridine. [b]$\Delta E_{1/2} = E_{1/2}(IV/III) - E_{1/2}(III,II)$ in millivolts. [c]$pK_{a,II}$ and $pK_{a,III}$ represent the pK_a of the corresponding $Ru^{II}OH_2$ and $Ru^{III}OH_2$ species, respectively. [d]TOF_i stands for the initial turnover frequency in cycles per second and TN for the turnover number. These values are extracted for the catalytic reactions involving 1.0 mM Cat/100 mM Ce^{IV} in a 0.1 M triflic acid solution with a total volume of 2 mL. [e]Tw means this work [f]Two-electron process.

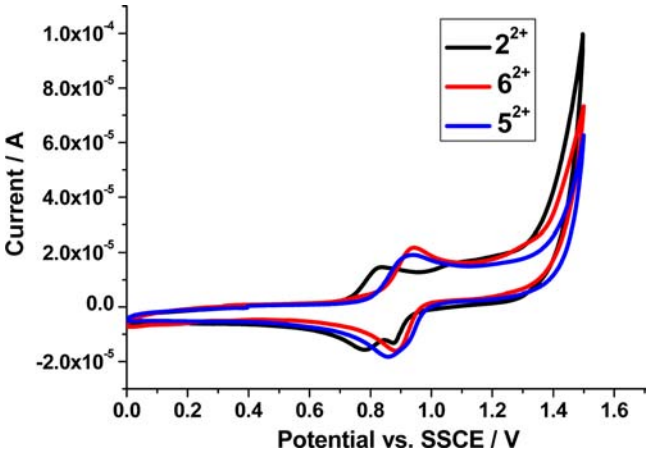

Figure 2. Cyclic voltammetry of 1 mM solutions in 0.1 M CF_3SO_3H (pH = 1.0) for complexes $\mathbf{2}^{2+}$ (black), $\mathbf{5}^{2+}$ (blue), and $\mathbf{6}^{2+}$ (red). Scan rate 100 mV s^{-1} using a glassy carbon working electrode, a platinum wire auxiliary electrode, and a SSCE reference electrode.

complexes their oxidation state III is unstable with regard to disproportion and thus a two-electron wave is found.

$$[Ru^{IV}{=}O]^{2+} + 2e^- + 2H^+ \rightarrow [Ru^{II}OH_2]^{2+} \quad (1)$$

E^o = 0.54 V for $\mathbf{5}^{2+}$ and 0.56 V for $\mathbf{6}^{2+}$ at pH = 7.0 (trpy and bpy ligands are not drawn). This is in sharp contrast to complex $\mathbf{2}^{2+}$,[6] where the two one-electron processes are separated by 110 mV. It is interesting to see here that the standard potential for the $Ru^{IV/II}$ couple for $\mathbf{2}^{2+}$ is practically identical with that of the fluorine complexes $\mathbf{5}^{2+}$ and $\mathbf{6}^{2+}$. This reveals that the presence of the F substituent in the bpy ligand produces an increase of the $Ru^{III/II}$ couple, as expected, for the electron-withdrawing properties of the F group but surprisingly produces a dramatic decrease of the IV/III redox potential. It is also important to realize here that the IV/II standard potentials for $\mathbf{5}^{2+}$ and $\mathbf{6}^{2+}$ differ merely by 20 mV and thus indicates that the direct contact of the F group with the aqua group, distorting slightly its geometry, practically does not affect the electronic structure of the metal center. A similar phenomenon is observed for the next redox couple corresponding to the oxidation of Ru^{IV} to Ru^{V}, where in this case the potentials for $\mathbf{5}^{2+}$ and $\mathbf{6}^{2+}$ differ now by only 10 mV (1.68 V for $\mathbf{5}^{2+}$ and 1.69 V for $\mathbf{6}^{2+}$). However, while for the two-electron-transfer process for $Ru^{IV/II}$ there is not much influence because of the opposite trend of the individual redox potentials just described, for the $Ru^{V/IV}$ standard potential, the F substituent produces an anodic shift of 60 to 70 mV for $\mathbf{5}^{2+}$ and $\mathbf{6}^{2+}$, respectively, with regard to the unsubstituted bpy complex $\mathbf{2}^{2+}$. As can be observed in Figure 2, this wave is accompanied by a large electrocatalytic current intensity associated with the oxidation of water to dioxygen. For the $\mathbf{2}^{2+}$ case, it is proposed that, right at this high oxidation state, O–O bond formation occurs, followed by a sequence of reactions that lead to the formation of dioxygen, as exemplified below (again trpy and bpy ligands are not shown),

$$[Ru^{V}{=}O]^{3+} + H_2O \rightarrow [Ru^{III}OOH]^{2+} + H^+ \quad (2)$$

$$[Ru^{III}OOH]^{2+} - 1e^- - 1H^+ \rightarrow [Ru^{IV}OO]^{2+} \quad (3)$$

$$[Ru^{IV}OO]^{2+} + H_2O \rightarrow [Ru^{II}OH_2]^{2+} + O_2 \quad (4)$$

and where the rate-determining step (rds) is proposed to be the last reaction (eq 4), where the release of oxygen is produced.[6b,c] The perturbation exerted by the presence of the F group in $\mathbf{5}^{2+}$ and $\mathbf{6}^{2+}$ is nicely perceived in their acidities at oxidation state II. Whereas $\mathbf{5}^{2+}$ decreases the $pK_{a,II}$ by 0.8 log units compared to $\mathbf{2}^{2+}$, as expected from the electron-withdrawing effect of the F substituent, $\mathbf{6}^{2+}$ causes the opposite effect, increasing the pK_a by 0.6 log units (see Table 1). The latter is attributed to hydrogen bonding in $\mathbf{6}^{2+}$, which stabilizes the $Ru^{II}OH_2$ species, as seen in Figures 1 (X-ray structure) and 4. Taking into account that both $\mathbf{5}^{2+}$ and $\mathbf{6}^{2+}$ isomers, according to the electrochemical data, have practically the same electronic effect over the metal center, this implies then that the hydrogen-bonding effect is responsible for the 1.4 log unit increase of the pK_a; that is, $\mathbf{6}^{2+}$ is roughly 25 times more basic than $\mathbf{5}^{2+}$.

The catalytic activity of complex $\mathbf{5}^{2+}$ and $\mathbf{6}^{2+}$ towards the oxidation of water to dioxygen was also evaluated and compared to the unsubstituted bpy complex $\mathbf{2}^{2+}$. Figure 3 presents the oxygen evolution profile obtained when 1 mM catalysts are treated with 100 mM cerium(IV) oxidant at pH = 1.0 in a triflic acid aqueous solution with a total volume of 2 mL. The oxygen generation was monitored manometrically, and the nature of the gases was also followed on line by mass spectrometry, indicating that no other gases were formed in the reaction. As can be observed in the graph, both the dioxygen generation initial rate (TOF_i) and the overall turnover number (TN; see Table 1) are strongly affected by the substituted F-bpy's compared to the unsubstituted ones. In the purely electronic scenario, which compares $\mathbf{2}^{2+}$ with $\mathbf{5}^{2+}$, the initial rate decreases by a factor near to 4 (15.1 vs 4.3). On the other hand,

dx.doi.org/10.1021/ic3028176 | Inorg. Chem. 2013, 52, 3591–3593

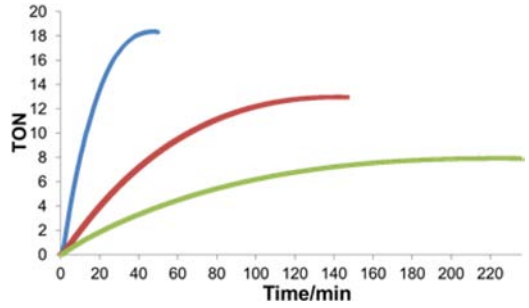

Figure 3. Dioxygen evolution versus time manometric profiles for catalysts $\mathbf{2}^{2+}$ (blue), $\mathbf{5}^{2+}$ (red), and $\mathbf{6}^{2+}$ (green) under 1:100 Cat/Ce^{IV} ratios in 0.1 M triflic acid solutions (pH = 1.0).

the purely hydrogen-bonding scenario, which compares $\mathbf{5}^{2+}$ and $\mathbf{6}^{2+}$, the initial rate decreases by a factor bigger than 2 (4.3 vs 1.7). Thus, because both factors operate in the same direction in the comparison of $\mathbf{2}^{2+}$ with $\mathbf{6}^{2+}$, the initial rate decreases by a factor of 9.

The 4 times decrease in TOF_i for the purely electronic effect exerted by $\mathbf{5}^{2+}$ with regard to $\mathbf{2}^{2+}$ indicates that eq 4 is no longer the rds because this is formally an intramolecular electron-transfer step where Ru^{IV} oxidizes the peroxide to dioxygen concomitant with its release; therefore, an increase in the standard potentials would suppose an increase in the rate. Indeed, a kinetic study based on the initial oxygen evolution velocities shows that the rate of the reaction is first-order in ruthenium and second-order in cerium (see the SI). This is consistent with a rds where the $[Ru^{IV}OO]^{2+}$ species is further oxidized to Ru^{V} (eq 6) preceded by a fast equilibrium step, as shown in eq 5,

$$[Ru^{V}{=}O]^{3+} + H_2O - 1e^- \rightleftarrows [Ru^{IV}OO]^{2+} + 2H^+ \quad (5)$$

$$[Ru^{IV}OO]^{2+} - 1e^- \rightarrow [Ru^{V}OO]^{2+}\ (\text{slow}) \quad (6)$$

followed by a fast release of dioxygen.

$$[Ru^{V}OO]^{3+} + H_2O \rightarrow [Ru^{III}OH_2]^{3+} + O_2\ (\text{fast}) \quad (7)$$

Finally, the fact that all of the standard potentials for $\mathbf{5}^{2+}$ and $\mathbf{6}^{2+}$ are practically identical contrasts with the 2 times decrease in TOF_i for $\mathbf{6}^{2+}$ with regard to that for $\mathbf{5}^{2+}$. This clearly points towards a potential stabilization of the $[Ru^{III}OOH]^{2+}$ (7) intermediate through hydrogen bonding, as shown in Figure 4. This stabilization produces a severe slowing down in the process, in line with the basicity increase described previously for the $pK_{a,II}$ for $\mathbf{6}^{2+}$, given the proton-coupled electron-transfer nature of the process.

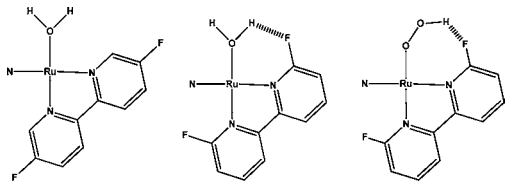

$\mathbf{5}^{2+}$ $\mathbf{6}^{2+}$ $\mathbf{7}^{+}$

Figure 4. Drawings of $\mathbf{5}^{2+}$, $\mathbf{6}^{2+}$, and $\mathbf{7}^{+}$ (trpy ligands are omitted except for the central N atom) showing the hydrogen interactions between the aqua and peroxo ligands with the F group of the bpy ligand, where appropriate.

In conclusion, careful ligand design of mononuclear tpry-bpy-Ru-aqua types of complexes allows one to understand how electronic perturbations and hydrogen-bonding interactions influence their water oxidation activity.

■ ASSOCIATED CONTENT

Ⓢ Supporting Information

X-ray crystallographic data in CIF format, additional experimental, spectroscopic, electrochemical, and kinetic data. This material is available free of charge via the Internet at http://pubs.acs.org.

■ AUTHOR INFORMATION

Corresponding Author

*E-mail: allobet@iciq.cat.

Notes

The authors declare no competing financial interest.

■ ACKNOWLEDGMENTS

Support from MINECO (CTQ2010-21497 and PRI-PIBIN-2011-1278) is gratefully acknowledged. S.M. thanks MINECO for a Torres Quevedo contract, and I.L. thanks MINECO for a FPU grant. CCDC 929406 and 929407 contain the supplementary crystallographic data for this paper. This data can be obtained free of charge via www.ccdc.cam.ac.uk/conts/retrieving.html (or from the Cambridge Crystallographic Data Centre, 12 Union Road, Cambridge CB21EZ, UK; (fax: (+44) 1223-336-033; or e-mail: deposit@ccdc.cam.ac.uk).

■ REFERENCES

(1) Zong, R.; Thummel, R. P. *J. Am. Chem. Soc.* **2005**, *127*, 12802−12803.

(2) Concepcion, J. J.; Jurss, J. W.; Templeton, J. L.; Meyer, T. J. *J. Am. Chem. Soc.* **2008**, *130*, 16462−16463.

(3) (a) Ellis, W. C.; McDaniel, N. D.; Bernhard, S.; Collins, T. J. *J. Am. Chem. Soc.* **2010**, *132*, 10990. (b) Wasylenko, D. J.; Palmer, R. D.; Schott, E.; Berlinguette, C. P. *Chem. Commun.* **2012**, *48*, 2107. (c) Chen, Z.; Concepcion, J. J.; Luo, H.; Hull, J. F.; Paul, A.; Meyer, T. J. *J. Am. Chem. Soc.* **2010**, *132*, 17670−17673. (d) Roeser, R.; Farras, P.; Bozoglian, F.; Martínez-Belmonte, M.; Benet-Buchholz, J.; Llobet, A. *ChemSusChem* **2011**, *4*, 197−207. (e) Blakemore, J. D.; Schley, N. D.; Balcells, D.; Hull, J. F.; Olack, G. W.; Incarvito, C. D.; Eisenstein, O.; Brudvig, G. W.; Crabtree, R. H. *J. Am. Chem. Soc.* **2010**, *132*, 16017−16029.

(4) Wasylenko, D. J.; Ganesamoorthy, C.; Henderson, M. A.; Koivisto, B. D.; Osthoff, H. D.; Berlinguette, C. P. *J. Am. Chem. Soc.* **2010**, *132*, 16094−16106.

(5) (a) Yamazaki, H.; Hakamata, T.; Komi, M.; Yagi, M. *J. Am. Chem. Soc.* **2011**, *133*, 8846−8849. (b) Boyer, J. L.; Polyansky, D. E.; Szalda, D. J.; Zong, R.; Thummel, R. P.; Fujita, E. *Angew. Chem., Int. Ed.* **2011**, *50*, 12600−12604.

(6) (a) Yoshida, M.; Masaoka, S.; Abe, J.; Sakai, K. *Chem.—Asian J.* **2010**, *5*, 2369−2378. (b) Concepcion, J.; Jurss, J. W.; Norris, M. R.; Chen, Z.; Templeton, J. L.; Meyer, T. J. *Inorg. Chem.* **2010**, *49*, 1277. (c) Wasylenko, D. J.; Ganesamoorthy, C.; Koivisto, B. D.; Henderson, M. A.; Berlinguette, C. P. *Inorg. Chem.* **2010**, *49*, 2202−2209. (d) Angeles-Boza, A. M.; Roth, J. P. *Inorg. Chem.* **2012**, *51*, 4722.

(7) Masllorens, E.; Rodríguez, M.; Romero, I.; Roglans, A.; Parella, T.; Benet-Buchholz, J.; Poyatos, M.; Llobet, A. *J. Am. Chem. Soc.* **2006**, *128*, 5306−5307.

(8) (a) Welch, T. W.; Ciftan, S. A.; White, P. S.; Thorp, H. H. *Inorg. Chem.* **1997**, *36*, 4812. (b) Vigara, L.; Ertem, M. Z.; Planas, N.; Bozoglian, F.; Leidel, N.; Dau, H.; Haumann, M.; Gagliardi, L.; Cramer, C. J.; Llobet, A. *Chem. Sci.* **2012**, *3*, 2576−2586.